# Numerical study of magnetic phase transitons and critical temperature in a ferromagnet using the 2D Ising model

Henrik Haug
Axl H Kleven
Live Ljungqvist Storborg

(Dated: September 22, 2025)

The understanding of magnetic phase transitions of a ferromagnet in different temperatures is an important field in theoretical physics with applications in electromagnetic appliances. The Ising model is a simple yet accurate model used to describe the phase transitions and critical temperatures of ferromagnets. It also serves many uses outside the study of ferromagnets, and is as such an important tool to get familiar with. As such, we have used the model to describe a 2D lattice of spins, to predict the phase transitions and critical temperature of a ferromagnet. Numerically, we use Markov Chain Monte Carlo methods with optimization methods like burn-in and parallelisation. For the $2 \times 2$ case we find analytical solutions, and when using 50'000 Monte Carlo cycles, we get a good agreement between the analytical and numerical results. The burn-in time for the $20 \times 20$ case was $10^5$ Monte Carlo cycles, such that $10^6$ Monte Carlo cycles is optimal. Using $10^6$ Monte Carlo cycles with lattice sizes of $40 \times 40, 60 \times 60, 80 \times 80,$ and $100 \times 100$ we study phase transitions and critical temperatures. For the $100 \times 100$ lattice, we observed a phase transition and estimated critical temperatures at $T_c = 2.279 \frac{J}{k_B}$ for $\frac{\chi}{N}$ and $T_c = 2.277 \frac{J}{k_B}$ for $\frac{C_v}{N}$. Utilizing these results, we used linear regression to estimate the critical temperature for an infinitely large lattice, finding it to be $T_c = 2.2529 \frac{J}{k_B} \pm 0.0026 \frac{J}{k_B}$. This result is $0.71\% \pm 0.26\%$ smaller than Lars Onsager's analytical value of $2.269 \frac{J}{k_B}$. This is very close, but further away than expected, with the analytical result not being within the error. Our result is likely to improve by using a more fine-grained analysis.

## I. INTRODUCTION

The Ising model was originally made to explain how materials become magnetic, which is mainly how we will use the model. The model is simple, using a grid of up or down states, which can only interact with its nearest neighbours. Despite its simplicity, the Ising model is highly accurate and applicable to real systems, explaining among other things phase transitions very well. Lars Onsager was for example able to use the Ising model to find the critical temperature for an infinite 2D lattice, which is an important result in theoretical physics. In addition to this, the model can be applied to understand complex systems such as neuroscience, social network analysis, and computational biology [1]. As such, the Ising model is an interesting tool to get familiar with, as its original appliances are important, and the possibility for other applications are grand.

We will test our numerical simulation by first studying the specific 2×2 lattice case, where the Ising model is analytically solvable. We will use these analytical results to compare with our numerical results for varying temperatures and iterations. For the whole article we will be considering the energy, magnetisation, heat capacity, and magnetic susceptibility when studying the system.

Our numerical simulation of the Ising model will use Markov Chain Monte Carlo methods, more specifically the Metropolis-Hastings algorithm, with certain analytical improvements available for the Ising model. And when increasing our lattice size we will require numerical optimization methods like burn-in, thinning, and parallelization. The results and implementation of these methods will be thoroughly tested and discussed.

For larger lattices we will be studying the magnetic phase transitions as a function of lattice sizes and temperature. For these we will also find the critical temperatures, before attempting to find the critical temperature of an infinite lattice size. We will compare this to Onsager's result. A real material would have a lattice size on the size of Avogadros number, and as such an infinite lattice would more closely resemble a real material.

## II. METHOD & THEORY

### A. Ising model

The Ising model is a mathematical model initially used to describe ferromagnetism using statistical mechanics [2]. The model describes a lattice of $N = L \times L$ discrete variables, here atomic (or particle) spins, which can be either up (+1) or down (-1), as shown in FIG 1. $L$ is the length of one side of the lattice. The spins $\mathbf{s}$ will be expressed mathematically as a vector

$$\mathbf{s} = (s_1, s_2, ..., s_N)$$

containing the spins of each particle $s_i$. The spins can affect each other, and when doing so it is only the nearest neighbours than can have an effect. When affected, the spins can change according to the Boltzmanz probability distribution function (pdf) shown in equation (1).

$$p(\mathbf{s}; T) = \frac{1}{Z} e^{-\beta E(\mathbf{s})}. \tag{1}$$

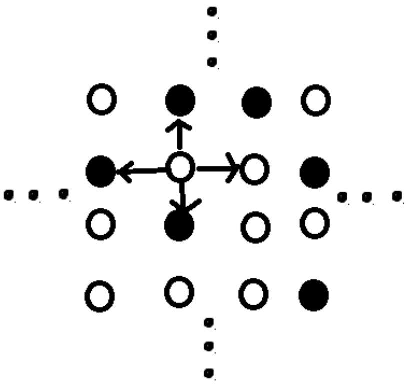

FIG. 1. The 2D Ising model is a lattice consisting of $L \times L$ particles with spins up (colored) or spins down (hollow). Each particle only interacts with the nearest neighbours.

This pdf is derived from thermodynamics, and is dependent on the temperature together with the partition function as shown in equation (2).

$$Z = \sum_{\text{All possible } \mathbf{s}} e^{-\beta E(\mathbf{s})}. \tag{2}$$

With $\beta$ defined in equation (3)

$$\beta = \frac{1}{k_B T}, \tag{3}$$

with the boltzmann constant $k_B = 1.380649 \cdot 10^{-23} \frac{\mathrm{m^2 kg}}{\mathrm{s^2 K}}$.

### 1. Physical properties

As mentioned, the Ising model describes ferromagnetism, and as such should have physical properties of a ferromagnet. We will be studying the total energy $E(\mathbf{s})$ and total magnetism $M(\mathbf{s})$ of the model, using equations (4), (5)

$$E(\mathbf{s}) = -J \sum_{\langle kl \rangle}^{N} s_k s_l, \tag{4}$$

$$M(\mathbf{s}) = \sum_{i}^{N} s_i. \tag{5}$$

Where $\sum_{\langle kl \rangle}^{N} s_k s_l$ means we count over all neighbouring pairs of spins without double counting. These equations are also derived from thermodynamics, and are interesting to study as we can study magnetism and phase transitions of a ferromagnet as a function of temperature and boundary conditions. Generally it is more interesting to study the total energy $\epsilon$ and magnetisation $m$ per spin, and to find these we simply divide by the number of spins. This is shown in equations (6), (7)

$$\epsilon(\mathbf{s}) = \frac{E(\mathbf{s})}{N}, \tag{6}$$

$$m(\mathbf{s}) = \frac{M(\mathbf{s})}{N}. \tag{7}$$

When numerically studying the Ising model we will apply periodic boundary conditions such that the lattice ‘wraps around’ and all spins have 4 adjacent spins: The last spin in a row or column of the lattice will be able to interact with the first. And vice versa. This will more resemble a real ferromagnet, where we in reality would have N amount of spins in the order of avogadros number, where the amount of boundary spins (only able to interact with 2 or 3 spins) would be very low compared to the total N.

Numerically, the periodic boundary conditions without double counting will be implemented by all particles only interacting with the particles below and to the right of themselves, with the border particles ‘looping around’ and interacting with the relevant particle on the opposite side.

For studying the phase transitions and critical temperature, we will be studying the heat capacity and magnetic susceptibility of the system. These quantities are dependent on the energy and magnetisation of the system. The critical temperature is a measure of heat required to change the temperature of the system. The critical temperature typically peaks around the phase transition, with the peak being the critical temperature. The magnetic susceptibility is a measure of how much the system responds to an external magnetic field, and behaves in a similar manner to the heat capacity.

## B. The 2x2 Lattice

The $2 \times 2$ Lattice of the Ising model with periodic boundary conditions has analytical solutions [1], which we will be using to later compare to the solutions of our numerical methods. The lattice can be represented in FIG 2. The lattice is here represented using either the spin up (+) and spin down (-), as well as denoting the spins using $S_1$, $S_2$, $S_3$, $S_4$. When considering the neighbouring pairs of spins without double counting, we thus get the following combinations. Without considering the boundary conditions:

$$(S_1, S_2), (S_1, S_3), (S_2, S_4), (S_3, S_4).$$

[1] In the $2 \times 2$ case, we technically double count when using periodic boundary conditions. The $2 \times 2$ case is however only used to test the code, and seeing as the periodic boundary conditions are an important part of the code, the periodic boundary conditions take priority.

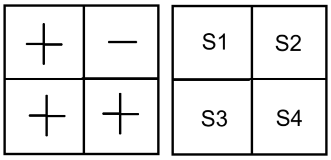

FIG. 2. The $2 \times 2$ Lattice using both the up (+) and down (-) (left), as well as the unknown spins $S_1$, $S_2$, $S_3$, $S_4$ notation.

| s + 1 | E | M | g |
|---|---|---|---|
| 4 | -8J | 4 | 1 |
| 3 | 0 | 2 | 4 |
| 2 | 0, 8J | 0 | 4, 2 |
| 1 | 0 | -2 | 4 |
| 0 | -8J | -4 | 1 |

TABLE I. s + 1 is the number of spins in the up state. E is the total energy. M is the total magnetisation. And g is the degeneracy.

And when considering the boundary conditions:

$$(S_1, S_2), (S_1, S_3), (S_2, S_4), (S_3, S_4).$$

We see that the contributions from the boundary conditions are the same as the contributions from with the lattice itself. Using these combinations together with equations (4), (5) we can easily calculate the energies and magnetisation of the different combinations of spins. The equations can now be written

$$E(\mathbf{s}) = -2J\left(S_1S_2 + S_1S_3 + S_2S_4 + S_3S_4\right), \qquad (8)$$

where we take advantage of the equality of the combinations with and without boundary conditions by multiplying by 2. The magnetisation are calculated by equation (5), which gives

$$M(\mathbf{s}) = S_1 + S_2 + S_3 + S_4, \qquad (9)$$

and these different combinations will also have degeneracies, as one can order the spins differently but still get the same energy. The amount of up spins, with their respective energies, magnetisations, and degeneracies are shown in TABLE I.

### 1. *Analytical expressions*

We here find analytical expressions for the $2 \times 2$ lattice that will come in useful when later testing the results of our code on the $2 \times 2$ case. We here find analytical expressions for: $Z, \langle\epsilon\rangle$, $\langle\epsilon^2\rangle$, $\langle|m|\rangle$, $\langle m^2\rangle$. Using these we can later calculate the variance, enabling us to also find the heat capacity $C_V(T)$ and magnetic susceptibility $\chi(T)$, both normalized to number of spins $N$. The calculations of these are presented in Appendix A, with the results being:

$$Z = 2e^{8\beta J} + 2e^{-8\beta J} + 12, \qquad (10)$$

$$\langle\epsilon\rangle = \frac{4J}{Z}\left(e^{-8\beta J} - e^{8\beta J}\right), \qquad (11)$$

$$\langle\epsilon^2\rangle = \frac{8J}{Z}\left(e^{-8\beta J} + e^{8\beta J}\right), \qquad (12)$$

$$\langle|m|\rangle = \frac{2}{Z}\left(e^{8\beta J} + 2\right), \qquad (13)$$

$$\langle m^2\rangle = \frac{2}{Z}\left(e^{8\beta J} + 1\right), \qquad (14)$$

$$\frac{C_V}{N} = \frac{32\beta J^2}{TZ}\left[e^{8\beta J} + e^{-8\beta J} - \frac{2}{Z}\left(e^{-16\beta J} - 2 + e^{16\beta J}\right)\right], \qquad (15)$$

$$\frac{\chi}{N} = \frac{8\beta}{Z}\left[e^{8\beta J} + 1 - \frac{2}{Z}\left(e^{16\beta J} + 4e^{8\beta J} + 4\right)\right]. \qquad (16)$$

## C. Markov Chain Monte Carlo

Markov Chain Monte Carlo (MCMC) methods are statistical methods used to approximate unknown pdfs. It does so by iteratively generating sample points using the probabilities of the system being studied, where the points are dependent on the previous points. As such, it produces a ‘chain’ (Markov chain) of points which resembles the unknown distribution. The method works for distributions of both high and low complexities, with different varieties like Gibbs sampler and Metropolis-Hastings being optimal for varying purposes. We have chosen the Metropolis-Hastings method due to the icing model representing a large and complex system, which the Metropolis-Hastings has been known to study efficiently.

### 1. *Metropolis-Hastings*

As previously mentioned, the Metropolis-Hastings method is a MCMC method used to approximate an unknown pdf. The method goes as shown in FIG 1, where the key point of the algorithm is the acceptance rule. The acceptance rule seeks to update the point $x_i$ in the Markov chain by always updating when the probability of the proposed point $x'$ is higher than the current. But also sometimes updating the point in the Markov chain when the probability of the proposed point is lower. This ensures a detailed and varied exploration of the pdf landscape, but also a clear probability distribution.

In the context of the Ising model, we will be randomly selecting spins in the lattice and proposing to flip its spin state according to the Boltzmann pdf (1). This will be the proposal pdf $T$. Our acceptance criterion $A$ will be dependent on the change in energy $\Delta E$ from flipping the spin, again using the probability of the given $\Delta E$ in the Boltzmann pdf (Here the $Z$ will cancel out when calculating the acceptance criterion and can be ignored). The

**Algorithm 1** The Metropolis-Hastings algorithm

```
Sample $x'$ according to $T(x_i \to x')$.
Calculate acceptance probability
    $$A\left(x_i \to x'\right) = \min\left(1, \frac{p(x')T(x' \to x_i)}{p(x_i)T(x_i \to x')}\right).$$
Which for symmetric proposal pdf's can be written as (the Metropolis algorithm)
    $$A\left(x_i \to x'\right) = \min\left(1, \frac{p(x')}{p(x_i)}\right).$$
Generate a random number r from $U(0,1)$.
  • If r $\leq A(x_i \to x')$:
      – $x_{i+1} = x'$.
  • If r $> A(x_i \to x')$:
      – $x_{i+1} = x_i$.
Repeat.
```

FIG. 3. The uniform distribution between 0 and 1 is denoted as $U(0,1)$. The Metropolis-Hastings algorithm always accepts a move to a state with higher probability, but can accept a move to a state with a lower probability.

acceptance or rejection of the state will still be dependent on the uniform distribution between 0 and 1. Seeing as the Boltzmann pdf is symmetric, we are technically applying the Metroplis method.

#### 2. *Analytical improvements*

In our MCMC we will need to calculate the boltzmann factor $e^{-\beta E(\mathbf{s})}$ for every spin in the lattice, for every iteration. This will be computationally expensive for high $L$. There is however a possibility to decrease this cost: Due to each spin only interacting with the nearest neighbours, the change in energy $\Delta E$ due to flipping a single spin $s_i$ in equation (17) has to take a set of discrete values

$$\Delta E = E_{\text{After}} - E_{\text{Before}}. \tag{17}$$

Where the energies before and after are shown in equations (18), (19), with an attempt to update the spin $s_i$ being made between calculating them.

$$E_{\text{Before}} = -Js_i \sum_{\langle kl \rangle} s_k s_l, \tag{18}$$

$$E_{\text{After}} = -Js_i \sum_{\langle kl \rangle} s_k s_l. \tag{19}$$

This gives a change in energy

$$\Delta E = Js_i \sum_{\langle kl \rangle} s_k s_l + Js_i \sum_{\langle kl \rangle} s_k s_l = 2Js_i \sum_{\langle kl \rangle} s_k s_l.$$

Where we know that the sum of the four neighbouring spins can take values $\{-4, -2, 0, 2, 4\}$. When all spins are negative we get -4, when 3 spins are negative and 1 is positive we get -2, and so on. This gives 5 possible changes in energy

$$\Delta E = \{-8J, -4J, 0J, 4J, 8J\}. \tag{20}$$

Which we use to increase the efficiency of our numerical calculations.

### D. Burn-in & thinning

Burn-in and thinning are techniques that are applied to increase accuracy and efficiency in a numerical model. Burn-in seeks to improve the accuracy of an MCMC method by removing the first steps in the Markov chain. The reasoning behind this is that the starting point of the Markov chain is highly unlikely, and over several iterations, the following points are more representative of the actual pdf. Thus, removing the initial points will give a more accurate approximation of the pdf, especially for fewer iterations. It is not necessarily always clear how many points should be removed, but one way to decide is to look at all the data points from the Markov chain, and study where the point seems to 'stabilize'. The amount of data points discarded is usually between 10% to 50% of the total amount of data points, depending on the data.

For a very large number of iterations, the Markov chain will become unnecessarily large and expensive on the memory. Thinning is employed to combat this, as it works by only saving an equally spaced portion of the data. It is common to save 5% to 20% of the data, depending on the size and variation in the data. A visual representation of burn-in together with thinning can be seen in FIG 4. In this figure we save 80% of the data, which is not truly representative of a real case. We did in fact not end up implementing thinning for this project due to us having enough memory for the chosen steps, as well as time-concerns.

### E. Testing and investigations

#### 1. *The 2x2 lattice, burn-in time, & the pdf*

For the 2 × 2 lattice we have analytical results for the following quantities, and will compare them to numerical results. We will compare $\langle \epsilon \rangle, \langle |m| \rangle, \frac{C_V}{N}, \frac{\chi}{N}$ using $T = 1.0\frac{J}{k_B}$ for different Monte Carlo cycles (1 Monte Carlo cycle = $N$ attempted flips). We here expect to get a very good agreement, and we wish to find how many Monte Carlo cycles we need to get the expected agreement. This will be a good indication that the code works as expected, and an indication of how many Monte Carlo cycles we will need.

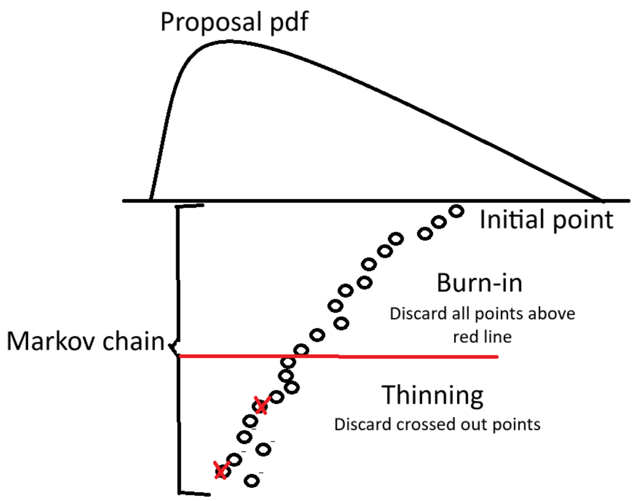

FIG. 4. Burn-in increases the accuracy of the approximated pdf by removing the first points of the Markov chain. Thinning improves on the unnecessary use of memory by removing equally spaced portions of the data.

To find the burn-in time we will be using a lattice size $L = 20$ to study $\epsilon$ and $\langle\epsilon\rangle$ at a range of Monte Carlo cycles for different temperatures. We will be using temperatures

- $T = 1.0\ \frac{J}{k_B}$ starting from an unordered state.
- $T = 1.0\ \frac{J}{k_B}$ starting from an ordered state.
- $T = 2.4\ \frac{J}{k_B}$ starting from an unordered state.
- $T = 2.4\ \frac{J}{k_B}$ starting from an ordered state.

Where an ordered state means all the spins are pointing the same way, and an unordered means the directions of the spins are randomly decided. This will allow us to decide the burn-in time for relevant temperatures, and how the initial state of the system affects the burn-in time.

We also expect the Metropolis-Hastings method to produce an approximation of a pdf for $\epsilon$. As such, creating a figure of the probability function using $T = 1.0\ \frac{J}{k_B}$ and $T$ $= 2.4\ \frac{J}{k_B}$ should produce a pdf. Finding this pdf will tell us more about the system, and using different temperatures will give us an indication of how the pdf changes over time.

### 2. Parallelization

For large lattice sizes, our calculations can become highly computationally expensive. To combat this we've parallelized parts of our code by using shared memory parallelization techniques. This takes use of multiple threads for calculating individual parts of the code simultaneously. For our calculations specifically, we parallelize our iteration over the different temperatures, using 4 threads instead of 1.

We calculate the MCMC by calculating the markov chains in parallel, and combining their results. In general we parallelized parts of our model where parallelization would increase efficiency, and give fast and correct results.

We test our parallelization by doing timing tests between the parallelized code and the serial code, to find the speed-up factor. To do this, we simply re-use the code made to produce the pdf's, as this calculation is fairly computationally expensive. We wish to find the relation between the time spent before and after parallelization.

### 3. Phase transitions & the infinite lattice

The magnetisation of the ferromagnet is temperature dependent, and as such, studying the magnetisation as a function of temperature is of interest. We thus wish to study $\langle\epsilon\rangle, \langle|m|\rangle, \frac{C_V}{N}, \frac{\chi}{N}$ as a function of temperature to study the phase change for different lattice sizes. For the lattice sizes we also wish to find the critical temperature (the temperature where the ferromagnet undergoes the phase change). This will be where the ferromagnet quickly changes magnetisation, and where we find the peaks of both the heat capacity and magnetic susceptibility. This is an important result for, among other things, super conductors. We find the critical temperatures by looking at an area around where we expect to find the critical temperatures, from our analytical results of the $2 \times 2$ case.

As previously mentioned, a real ferromagnet would have an N on the order of Avogadros number, and as such, considering a lattice of $L = \infty$ is of great interest for potential real world appliances. To study this, we will find the critical temperatures of different $L$, and use the scaling relation in equation (21)

$$T_c(L) - T_c(L = \infty) = aL^{-1} \tag{21}$$

to find an estimate for $T_c(L = \infty)$. Here, a is a constant we find by linear regression of the critical temperatures we found previously. Here we can do an error calculation using the mean square error (MSE) and R$^2$ score. An optimal MSE is 0, while an optimal R$^2$ score is 1.

## F. Tools

For our code we have used github, and our code can be found here [3]. Our code is mainly written in C++ where we have used the additional Armadillo [4] library. For creating figures we have used Python, with the following libraries: matplotlib [5], and numpy [6]. For linear regression we used scikit learns [7] functionality. For parallelisation we use OpenMP [8].

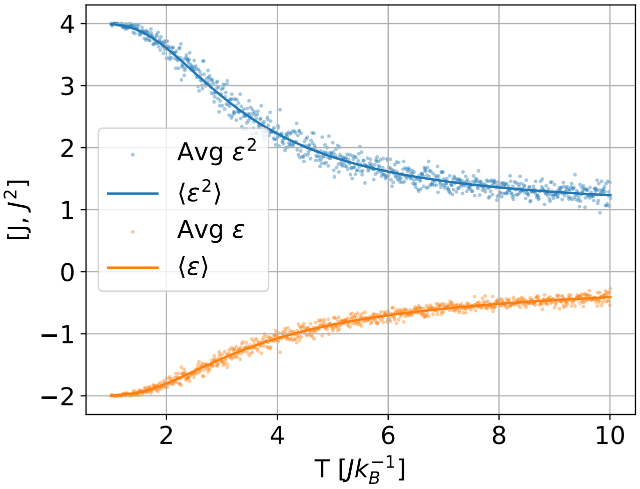

FIG. 5. Average energy per spin over 500 Monte Carlo cycles as a function of temperature, with the analytical results to compare.

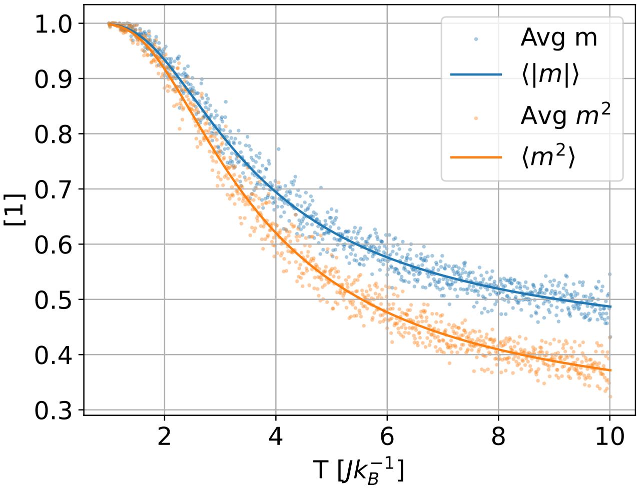

FIG. 6. Average magnetisation per spin over 500 Monte Carlo cycles as a function of temperature, with the analytical results to compare.

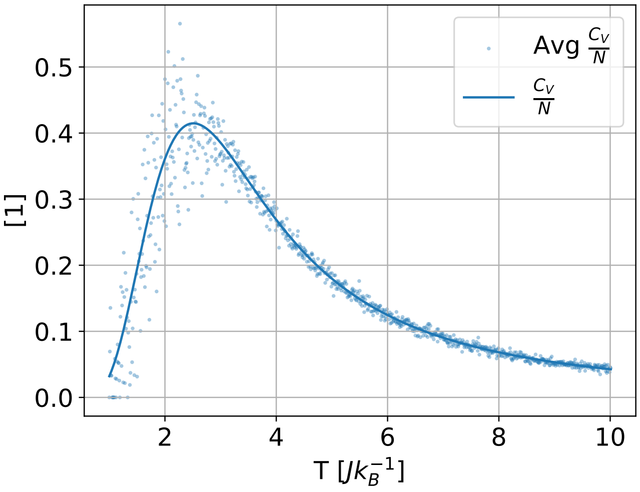

FIG. 7. Average heat capacity per spin over 500 Monte Carlo cycles as a function of temperature, with the analytical results to compare.

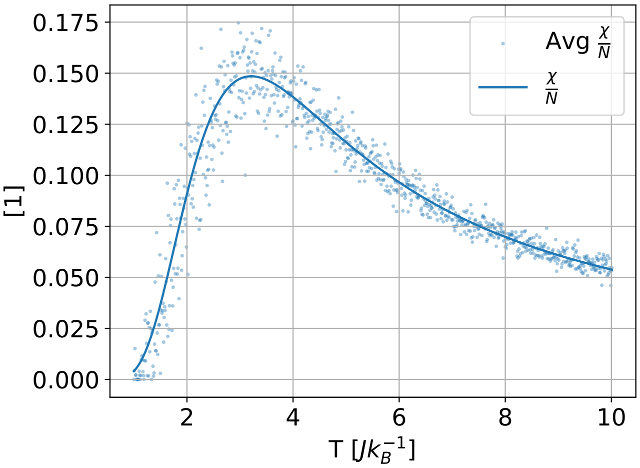

FIG. 8. Average magnetic susceptibility per spin over 500 Monte Carlo cycles as a function of temperature, with the analytical results to compare.

## III. RESULTS & DISCUSSION

### A. 2x2 Lattice

When using 500 Monte Carlo cycles for the $2\times 2$ lattice in FIG 5, 6, 7, 8 we see that there is a lot of noise, but the results are centered around the analytical results. This is a hint that our code is working as expected. The noise is larger for $C_V$ and $\chi$, which is also expected, as they are a scaling of the variance, which is dependent on the squares of $\epsilon$ and $m$.

When increasing the number of Monte Carlo cycles to 50'000 in FIG 9, 10, 11, 12, we can see a clear decrease in noise, and our numerical results now fit the analytical results very well. This is another clear indicator that our code works as expected. Further increasing the number of Monte Carlo cycles is expected to produce more and more accurate results at the expense of computational power.

Already here we can see a clear indication of a phase transition and a critical temperature. In the area $T \in [2,4]$ We see a sharp change in the magnetisation, suggesting a phase change from a magnetised to a non-magnetised state. And both the heat capacity and magnetic susceptibility show clear peaks around $T = 3$. This would indicate a critical temperature around $T = 3$. The peak in heat capacity is however at a slightly lower temperature than for magnetic susceptibility, and as such the critical temperature is not exactly the same for both

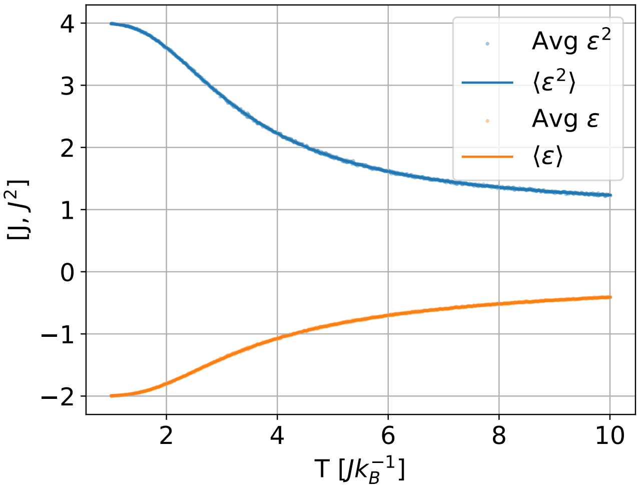

FIG. 9. Average energy per spin over 50'000 Monte Carlo cycles as a function of temperature, with the analytical results to compare.

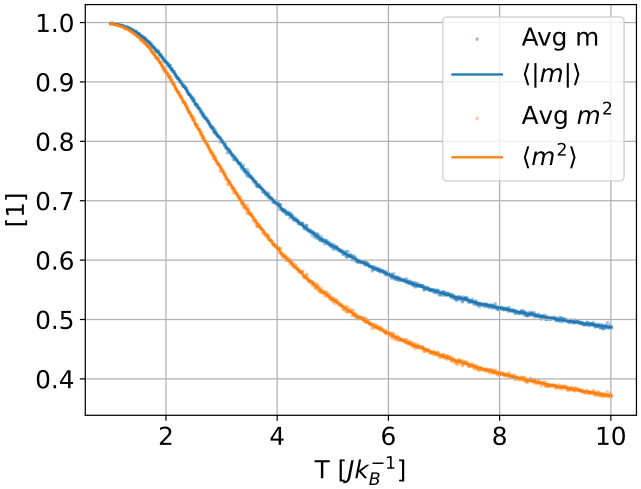

FIG. 10. Average magnetisation per spin over 50'000 Monte Carlo cycles as a function of temperature, with the analytical results to compare.

quantities.

### 1. Burn-in

Iterating over $10^6$ Monte carlo cycles, we get FIG 13, 14. Where we can see that the graphs stabilize around a certain value around $10^5$ Monte Carlo cycles, and as such the burn-in time for $L = 20$ is $10^5$ Monte Carlo cycles. This applies to both figures. As such, an optimal amount of Monte Carlo cycles appears to be $10^6$ using 10% Burn-in. This may vary using different $L$, as we saw that 50'000 steps produced a good result for the $2 \times 2$ case. We can also see that $10^6$ Monte Carlo cycles should

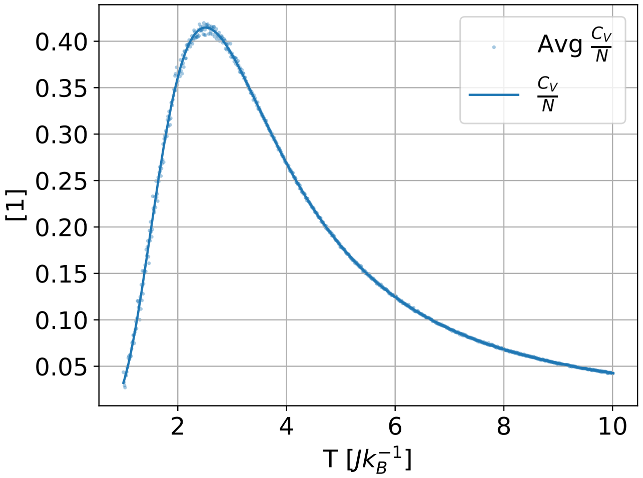

FIG. 11. Average heat capacity per spin over 50'000 Monte Carlo cycles as a function of temperature, with the analytical results to compare.

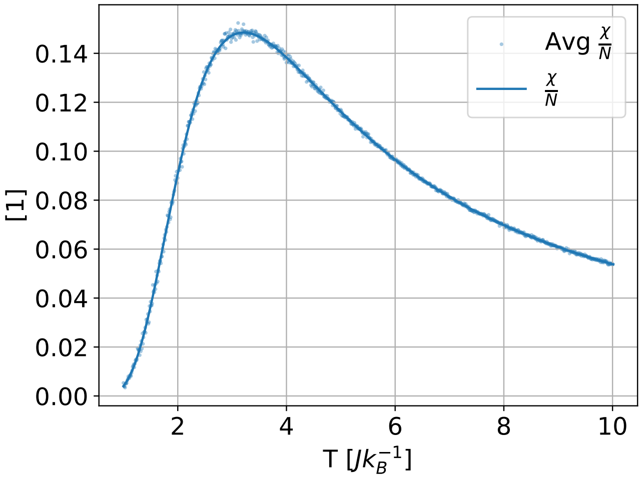

FIG. 12. Average magnetic susceptibility per spin over 50'000 Monte Carlo cycles as a function of temperature, with the analytical results to compare.

produce reliable results even if the burn-in is not optimal for other $L$, as we are sufficiently close to a stabilisation.

For the case of $T = 1.0\frac{J}{k_B}$ we can clearly see that the ordered state already starts at the peak of the pdf, as $\epsilon$ doesn't change. For the unordered state we see however that $\epsilon$ quickly drops down to around $-1.75J$, where it almost stabilizes, before dropping down to $-2.0J$ where it agrees with the ordered state. This stabilization at $-1.7J$ is unexpected, and could point towards there being two peaks in the actual pdf.

For the case of $T = 2.4\frac{J}{k_B}$ we see however that $\epsilon$ of neither the unordered nor the ordered state start out at the peak of the pdf. They both converge around $-1.75J$. As such, we can see that the energy of the system increases when we increase the temperature, which follows

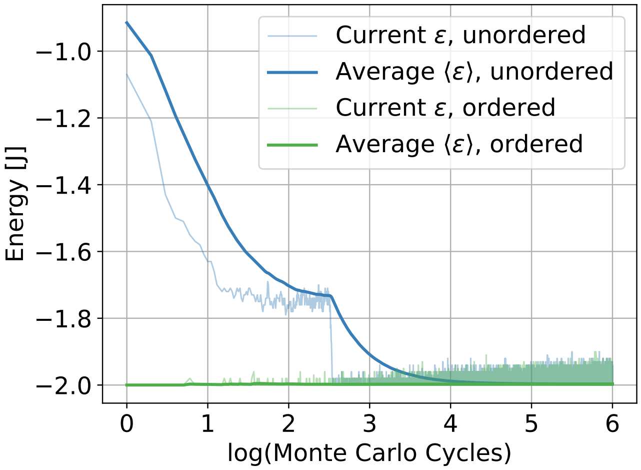

FIG. 13. Using $T = 1.0\frac{J}{k_B}$. The average expected energy per spin $\langle\epsilon\rangle$, using all the previous $\epsilon$ up to the current step. And the current $\epsilon$ of the given Monte Carlo step. Using ordered and unordered initial state.

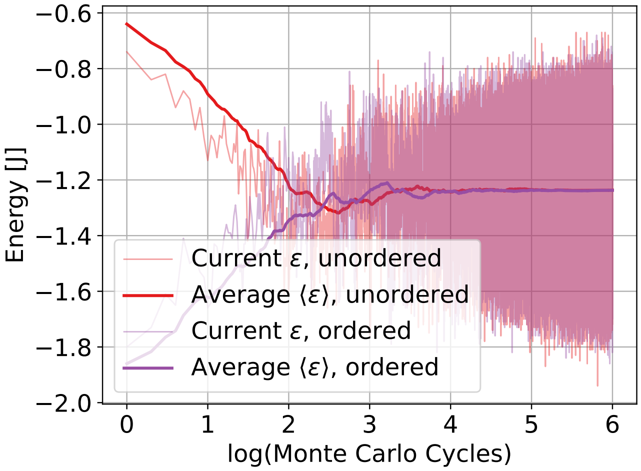

FIG. 14. Using $T = 2.4\frac{J}{k_B}$. The average expected energy per spin $\langle\epsilon\rangle$, using all the previous $\epsilon$ up to the current step. And the current $\epsilon$ of the given Monte Carlo step. Using ordered and unordered initial state.

expectation and points to a positive heat capacity being correct.

Further comparing the graphs, we see that the case of $T = 1.0\frac{J}{k_B}$ has way lower ‘noise’ than the $T = 2.4\frac{J}{k_B}$ case. This could point to the pdf being sharper.

### 2. *Pdf of energy per spin*

Iterating over $10^6$ Monte carlo cycles with 10% burn-in as we found in the previous results, we get FIG 15. Here we can see that the $T = 1.0\frac{J}{k_B}$ case has a peak on $-2.0J$, which corresponds to the value the graphs stabilized to in FIG 13. The $T = 2.4\frac{J}{k_B}$ case has a peak around $-1.25J$, which again corresponds to where the graphs stabilized in FIG 14. As such, the results agree with each other and the code appears correct.

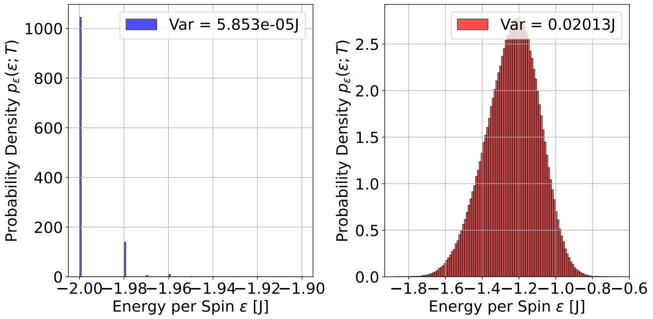

FIG. 15. Using $10^6$ Monte Carlo cycles with 10% burn-in we find the pdf of $\epsilon$ for $T = 1.0\frac{J}{k_B}$ and $T = 2.4\frac{J}{k_B}$.

For the pdf’s, we can clearly see that the $T = 1.0\frac{J}{k_B}$ case has two peaks, explaining the result of the two stabilizations in FIG 13. Otherwise, this case has a variance of $5.853 \cdot 10^{-5}J$. This variance is way smaller than the variance for the $T = 2.4\frac{J}{k_B}$ case, which is $0.02013J$. This can be seen visually by the pdf of $T = 2.4\frac{J}{k_B}$ being more evenly distributed. This difference in variance will explain the difference in noise between FIG 13, 14. Again, this points to our code being correct.

### 3. *Parallelisation*

Parallelising our code, and timing the calculation of the pdf’s produced in FIG 15, we get the following times. Serial: 133.869s, parallelised: 113.239s, giving a speed-up factor

$$\frac{133.869\text{s}}{113.239\text{s}} = 1.18218 \approx 1.18,$$

which is approximately an 18% increase in computational efficiency.

We chose to not parallelize the code to its full potential to ensure avoidance of race conditions, where threads try to access and modify the same data at the same time, resulting in wrong results. Our code experiences suboptimal performance due to load imbalance between threads. Some threads will have heavier workloads due to varying lattice sizes. Another impact of parallelization is overhead resulting from spawning and forking threads before and after the parallel regions. This overhead is negligible because of the necessity of parallelization.

### 4. *Phase transitions and critical temperatures*

We know that increasing $L$ will give create higher and higher peaks for $C_V$ and $\chi$ around the critical temperature. Following the results for the $2 \times 2$ case, we use

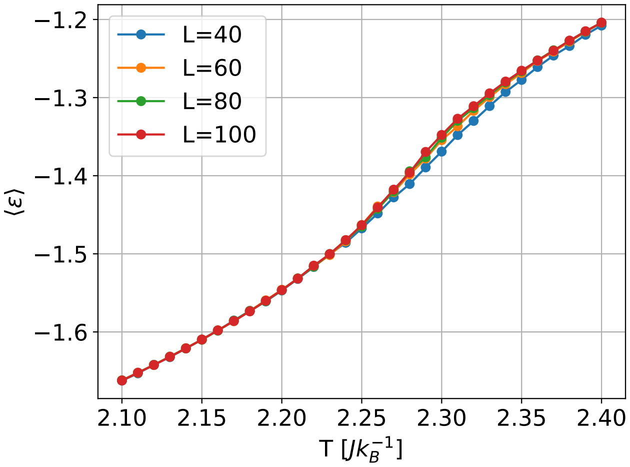

FIG. 16. Energy per spin for varying $L$ as a function of temperature using $10^6$ Monte Carlo cycles.

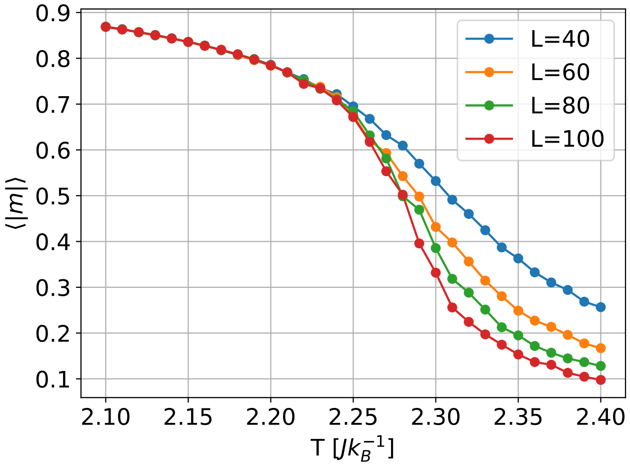

FIG. 17. Magnetisation per spin for varying $L$ as a function of temperature using $10^6$ Monte Carlo cycles.

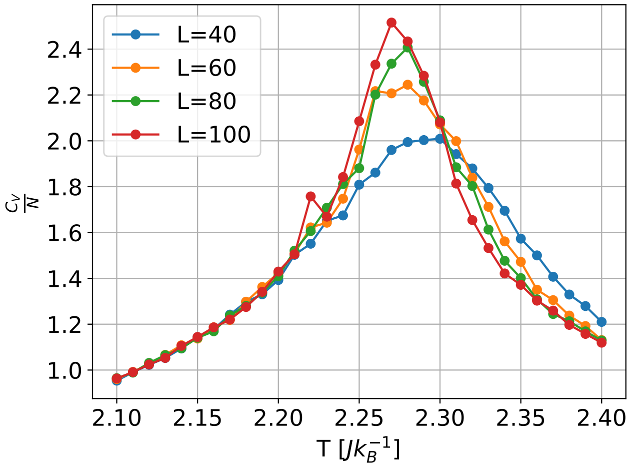

FIG. 18. Heat capacity per spin for varying $L$ as a function of temperature using $10^6$ Monte Carlo cycles.

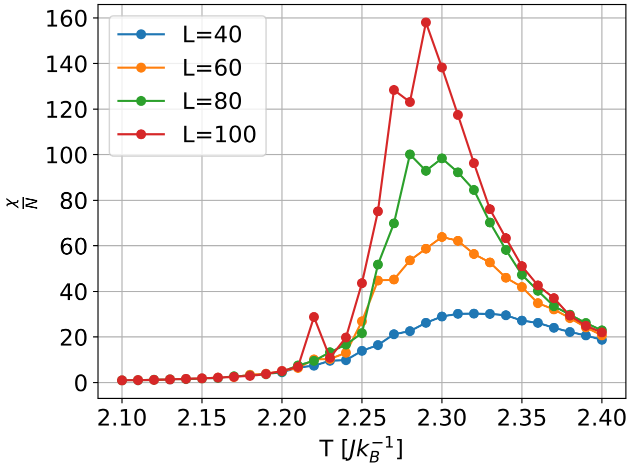

FIG. 19. Magnetic susceptibility per spin for varying $L$ as a function of temperature using $10^6$ Monte Carlo cycles.

a temperature $T \in [2.1, 2.4]\frac{J}{k_B}$ with a step of $0.01\frac{J}{k_B}$, and following the results of the burn-in we use $10^6$ Monte Carlo cycles. A smaller step would be more optimal, but this was too computationally expensive. Using $L = 40, 60, 80, 100$ to study $\langle\epsilon\rangle$, $\langle|m|\rangle$, $\frac{C_V}{N}$, $\frac{\chi}{N}$, we get FIG 16, 17, 18, 19, respectively. In these figures we can clearly see peaks in the heat capacity and magnetic susceptibility around $T = 2.275\frac{J}{k_B}$. This is a clear indication of a phase transition. For the magnetisation we can also see a clear drop around $T = 2.275\frac{J}{k_B}$, indicating a magnetic phase transition. For this temperature, the rate of increase for the energy also has a clear increase. In all the graphs we can clearly see that when increasing $L$, the peaks become higher and sharper, and the drop in magnetisation becomes sharper. We can also tell that the peaks are 'moving' towards lower temperatures, and as such our best estimation of the critical temperature is using the $L = 100$ case. Here, by looking at the magnetic susceptibility we get a critical temperature $T_c = 2.277\frac{J}{k_B}$, and for the heat capacity $T_c = 2.279\frac{J}{k_B}$.

The critical temperatures using both $\frac{C_V}{N}$ and $\frac{\chi}{N}$, for all cases of $L$ are shown in TABLE II. Where we can see that the critical temperatures for the heat capacity are consistently smaller than for the magnetic suscepti-

| L | $T_c$, $\frac{C_V}{N}$ $\left[\frac{J}{k_B}\right]$ | $T_c$, $\frac{\chi}{N}$ $\left[\frac{J}{k_B}\right]$ |
|---|---|---|
| 40 | 2.3 | 2.32 |
| 60 | 2.28 | 2.3 |
| 80 | 2.28 | 2.28 |
| 100 | 2.27 | 2.29 |

TABLE II. The critical temperatures (temperature of peak in the graph) from FIG 18, 19, for the different $L$.

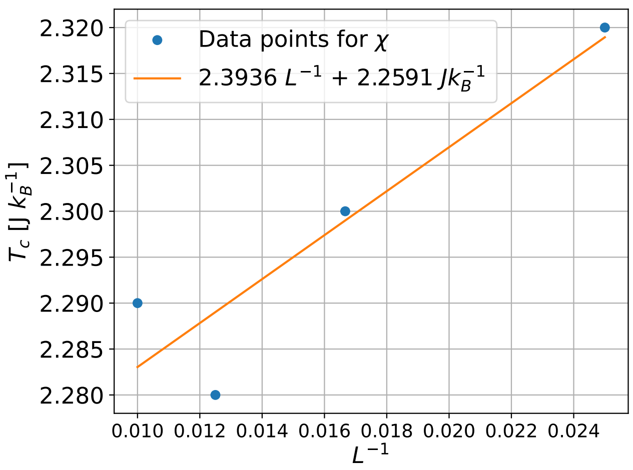

FIG. 20. Linearly regressing the critical temperatures for $\frac{\chi}{N}$ found in TABLE II to find an estimate of $T_C(L = \infty)$ using the scaling relation in equation (21).

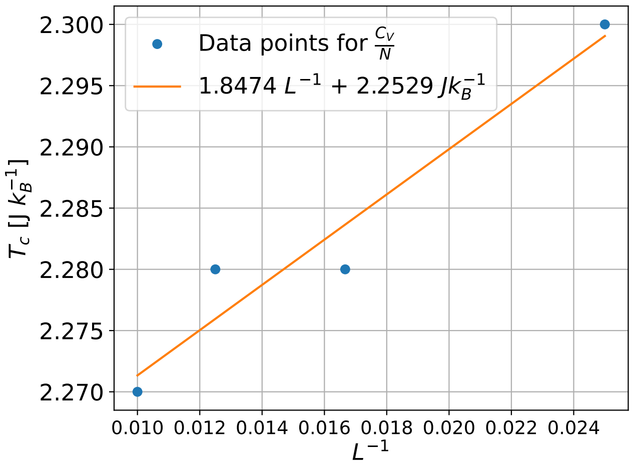

FIG. 21. Linearly regressing the critical temperatures for $\frac{C_v}{N}$ found in TABLE II to find an estimate of $T_C(L = \infty)$ using the scaling relation in equation (21).

bility, on the order of $10^{-2}$ (our step size). We would here expect them to have the same critical temperature for the same $L$, and considering the order of magnitude of disagreement, this is likely a restriction from the model, due to the lattice sizes being small in comparison to a real material. Again we can also see both critical temperatures becoming smaller as $L$ becomes bigger, and as such we expect a real critical temperature smaller than these values.

We linearly regress the critical temperatures in TABLE II to find an estimate of $T_c(L = \infty)$. This is visualised in FIG 20, 21. In these figures we are interested in the intercept, as this is where $L = \infty$. For $\frac{\chi}{N}$ the critical temperature is thus $T_c = 2.2591\frac{J}{k_B} \pm 0.0121\frac{J}{k_B}$ with the uncertainty being calculated by MSE. The result has an R$^2$ score of 0.8491. For $\frac{C_V}{N}$ the critical temperature is thus $T_c = 2.2529\frac{J}{k_B} \pm 0.0060\frac{J}{k_B}$. With an R$^2$ score of 0.9318. These results agree very well with each other, and both have good $MSE$ and R$^2$ scores, suggesting they are both good results.

The critical temperature calculated using $\frac{C_V}{N}$ has the least uncertainty with the best R$^2$, and is thus our best result. We compare this to Onsager's result:

$$\frac{2.2529\frac{J}{k_B}}{2.269\frac{J}{k_B}} \pm \frac{0.0060\frac{J}{k_B}}{2.269\frac{J}{k_B}} = 0.9929 \pm 0.0026.$$

As such, our result is $1 - 0.9929 = 0.71\% \pm 0.26\%$ smaller than Onsager's result. This is very close, but further away than expected, as the expected result is not within our error. This is likely caused by not using a fine-grained analysis of the temperature around the expected critical temperature. We attempted doing a fine-grain analysis, but this was too computationally expensive given our time frame. If we had access to either more computational power or time, we would thus expect our result to agree even better with Onsager's.

### *5. Further studies*

As mentioned, the Ising model was first made to study ferromagnetism, but now finds its way into appliances in many other fields. If we were given more time and inspiration, we would highly consider the application of the Ising model both for different materials and types of phase transitions, like water to ice. But also in fields outside of physics where a system can be reduced to a lattice of particles interacting with its neighbours, for example: Epidemiology, mapping the spread of new viruses by swapping the particles with people who are either ill or healthy. Or studying overfishing by swapping the particles with fish or fishermen. Both of these cases could potentially benefit from having 'moving' particles in the lattice, which would however increase complexity and sacrifice numerical efficiency.

## IV. CONCLUSION

Studying magnetic phase transitions in ferromagnets is an important topic in theoretical physics. The phase transitions can be understood using the Ising model, which is known for its simplicity and accuracy. The Ising model is also a valuable tool in other contexts and fields, and understanding the model itself has been an important part of our work. In our work, we have described a 2D lattice of spins, predicting the phase transitions and critical temperatures of ferromagnets using numerical methods. The numerical methods implemented were Markov Chain Monte Carlo methods along with optimization techniques such as burn-in, thinning, and parallelisation. Further, we found analytical results for the $2 \times 2$ lattice, where we experienced numerical results agreeing well with the analytical after 50'000 Monte Carlo cycles. For the larger $20 \times 20$ lattice, an optimal burn-in time was found to be $10^5$ making $10^6$ steps optimal. Therefore, we used $10^6$ Monte Carlo cycles for lattice sizes of $40 \times 40$, $60 \times 60$, $80 \times 80$, and $100 \times 100$ to study phase transitions and critical temperatures. For the $100 \times 100$ lattice, we observed a phase transition and estimated critical temperatures at $T_c = 2.29\frac{J}{k_B}$ for $\frac{\chi}{N}$ and $T_c = 2.27\frac{J}{k_B}$ for $\frac{C_v}{N}$. Utilizing these results, we used linear regression to estimate the critical temperature for an infinitely large lattice, finding it to be $T_c = 2.2529\frac{J}{k_B} \pm 0.0026\frac{J}{k_B}$. This result is $0.71\% \pm 0.26\%$ smaller than Lars Onsager's analytical value of $2.269\frac{J}{k_B}$. This is very close, but further away than expected, with the analytical result not being within the error. Our result is likely to improve by using a more fine-grained analysis.

[1] A. Lipowski, Ising model: Recent developments and exotic applications, last accessed 15 of november 2024.

[2] Wikipedia, Ising model, last accessed 14 of november 2024.

[3] H. Haug, A. H. Kleven, and L. L. Storborg, Project 4.

[4] R. C. Conrad Sanderson, Armadillo: a template-based c++ library for linear algebra., Journal of Open Source Software **1**, 7 (2016).

[5] J. D. Hunter, Matplotlib: A 2d graphics environment, Computing in Science & Engineering **9**, 90 (2007).

[6] C. R. Harris, K. J. Millman, S. J. van der Walt, R. Gommers, P. Virtanen, D. Cournapeau, E. Wieser, J. Taylor, S. Berg, N. J. Smith, R. Kern, M. Picus, S. Hoyer, M. H. van Kerkwijk, M. Brett, A. Haldane, J. F. del Río, M. Wiebe, P. Peterson, P. Gérard-Marchant, K. Sheppard, T. Reddy, W. Weckesser, H. Abbasi, C. Gohlke, and T. E. Oliphant, Array programming with NumPy, Nature **585**, 357 (2020).

[7] F. Pedregosa, G. Varoquaux, A. Gramfort, V. Michel, B. Thirion, O. Grisel, M. Blondel, P. Prettenhofer, R. Weiss, V. Dubourg, J. Vanderplas, A. Passos, D. Cournapeau, M. Brucher, M. Perrot, and E. Duchesnay, Scikit-learn: Machine learning in Python, Journal of Machine Learning Research **12**, 2825 (2011).

[8] R. Chandra, L. Dagum, D. Kohr, R. Menon, D. Maydan, and J. McDonald, *Parallel programming in OpenMP* (Morgan kaufmann, 2001).

## Appendix A: Analytical calculations for 2x2 lattice

Starting with Z, we remember equation (2) together with the energies and their degeneracies from TABLE I. We thus get

$$\begin{aligned} Z &= e^{-\beta(-8J)} + 4e^{-\beta(0)} + 4e^{-\beta(0)} \\ &\quad + 2e^{-\beta(8J)} + 4e^{-\beta(0)} + e^{-\beta(-8J)} \\ &= e^{8\beta J} + 4 + 4 + 2e^{-8\beta J} + 4 + e^{8\beta J} \\ &= 2e^{8\beta J} + 2e^{-8\beta J} + 12. \end{aligned} \tag{A1}$$

Continuing with $\langle \epsilon \rangle$ we can write this as

$$\langle \epsilon \rangle = \frac{\langle E(\mathbf{s}) \rangle}{N}.$$

In this case N = 4 because we have 4 spins. We apply the definition of an expectation value as shown in equation (A2).

$$\langle f(x) \rangle = \sum f(x) P(x). \tag{A2}$$

Where $\langle f(x) \rangle$ is the expectation value of a function of a discrete variable x with a probability $P(x)$. Together with the degeneracies of the energies from TABLE I, the expectation value of the energy becomes

$$\begin{aligned} \langle E \rangle &= \sum E(\mathbf{s}) P(\mathbf{s}) \\ &= \frac{1}{Z}\left(-8Je^{8\beta J} + 2 \cdot 8Je^{-8\beta J} - 8Je^{8\beta J}\right) \\ &= \frac{1}{Z}\left(-16Je^{8\beta J} + 16Je^{-8\beta J}\right) \\ &= \frac{16J}{Z}\left(e^{-8\beta J} - e^{8\beta J}\right). \end{aligned}$$

Where we use Z as found in equation (A1). This gives the analytical expression for $\langle \epsilon \rangle$ in equation (A3).

$$\begin{aligned} \langle \epsilon \rangle &= \frac{16J}{4Z}\left(e^{-8\beta J} - e^{8\beta J}\right) \\ &= \frac{4J}{Z}\left(e^{-8\beta J} - e^{8\beta J}\right). \end{aligned} \tag{A3}$$

We calculate $\langle \epsilon^2 \rangle$ in a similar fashion

$$\langle \epsilon^2 \rangle = \frac{\langle E(\mathbf{s})^2 \rangle}{N^2}.$$

With

$$\begin{aligned} \langle E^2 \rangle &= \sum E(\mathbf{s})^2 P(\mathbf{s}) \\ &= \frac{1}{Z}\left((8J)^2 e^{8\beta J} + 2 \cdot (-8J)^2 e^{-8\beta J} + (8J)^2 e^{8\beta J}\right) \\ &= \frac{1}{Z}\left(64J^2 e^{8\beta J} + 2 \cdot 64J^2 e^{-8\beta J} + 64J^2 e^{8\beta J}\right) \\ &= \frac{128J^2}{Z}\left(e^{8\beta J} + e^{-8\beta J}\right). \end{aligned}$$

Giving the analytical expression for $\langle \epsilon^2 \rangle$ in equation (A4).

$$\begin{aligned} \langle \epsilon^2 \rangle &= \frac{128J^2}{4^2 Z}\left(e^{8\beta J} + e^{-8\beta J}\right) \\ &= \frac{8J^2}{Z}\left(e^{8\beta J} + e^{-8\beta J}\right). \end{aligned} \tag{A4}$$

We take the absolute value of m before finding the expectation value, as the direction of the magnetisation (+ or -) is simply a matter of flipping the lattice and is irrelevant. The expectation value can thus be written

$$\langle |m| \rangle = \frac{\langle |M(\mathbf{s})| \rangle}{N}.$$

Where $\langle |M(\mathbf{s})| \rangle$ is found in a similar fashion to $\langle E(\mathbf{s}) \rangle$, using equations (A2), (1), together with the degeneracies for the magnetisations from TABLE I, giving

$$\begin{aligned}\langle |M(\mathbf{s})| \rangle &= \frac{1}{Z}(|4|e^{-8\beta J} + |2| \cdot 4 \cdot e^0 \\ &+ |-2| \cdot 4 \cdot e^0 + |-4| \cdot e^{-8\beta J}) \\ &= \frac{1}{Z}\left(8e^{8\beta J} + 16\right) \\ &= \frac{8}{Z}\left(e^{8\beta J} + 2\right).\end{aligned}$$

Which gives the analytical expression in equation (A5)

$$\begin{aligned}\langle |m| \rangle &= \frac{8}{4Z}\left(e^{8\beta J} + 2\right) \\ &= \frac{2}{Z}\left(e^{8\beta J} + 2\right).\end{aligned} \tag{A5}$$

We calculate $\langle m^2 \rangle$ in a similar fashion

$$\langle m^2 \rangle = \frac{\langle M(\mathbf{s})^2 \rangle}{N^2}.$$

With

$$\begin{aligned}\langle M(\mathbf{s})^2 \rangle &= \frac{1}{Z}(16e^{8\beta J} + 4 \cdot 4 \cdot e^0 \\ &+ 4 \cdot 4 \cdot e^0 + 16e^{8\beta J}) \\ &= \frac{1}{Z}(32e^{8\beta J} + 32) \\ &= \frac{32}{Z}(e^{8\beta J} + 1).\end{aligned}$$

Giving the analytical expression in equation (A6)

$$\begin{aligned}\langle m^2 \rangle &= \frac{32}{4^2 Z}\left(e^{8\beta} + 1\right) \\ &= \frac{2}{Z}\left(e^{8\beta} + 1\right).\end{aligned} \tag{A6}$$

From Thermodynamics we know that the heat capacity $C_V(T)$ can be written as equation (A7)

$$C_V(T) = \frac{1}{k_B T^2}\mathrm{Var}(E) = N^2 \frac{1}{k_B T^2}\mathrm{Var}(\epsilon). \tag{A7}$$

Where the variance is defined in equation (A8)

$$\mathrm{Var}(x) = \langle x^2 \rangle - \langle x \rangle^2. \tag{A8}$$

Using this in equation (A7), we get equation (A9) for the heat capacity normalised to number of spins

$$\begin{aligned}\frac{C_V(T)}{N} &= \frac{1}{N}\frac{1}{k_B T^2}\left[\langle E^2 \rangle - \langle E \rangle^2\right] \\ &= N\frac{1}{k_B T^2}\left[\langle \epsilon^2 \rangle - \langle \epsilon \rangle^2\right].\end{aligned} \tag{A9}$$

Using this together with our previous results we can rewrite this equation, as shown in (A10).

$$\begin{aligned}\frac{C_V(T)}{N} &= \frac{4\beta}{T}\left[\frac{8J^2}{Z}\left(e^{8\beta J} + e^{-8\beta J}\right) - \left(\frac{4J}{Z}\left(e^{-8\beta J} - e^{8\beta J}\right)\right)^2\right] \\ &= \frac{32\beta J^2}{T}\frac{1}{Z}\left[\left(e^{8\beta J} + e^{-8\beta J}\right) - \frac{2}{Z}\left(e^{-16\beta J} - 2e^0 + e^{16\beta J}\right)\right] \\ &= \frac{32\beta J^2}{TZ}\left[e^{8\beta J} + e^{-8\beta J} - \frac{2}{Z}\left(e^{-16\beta J} - 2 + e^{16\beta J}\right)\right].\end{aligned} \tag{A10}$$

Further we can in a similar fashion define the magnetic susceptibility $\chi(T)$ in equation (A11)

$$\chi(T) = \frac{1}{k_B T}\mathrm{Var}(M) = N\frac{1}{k_B T}\mathrm{Var}(m). \tag{A11}$$

Which, using the definition of the variance from equation (A8) gives equations (A12), (A13) for the magnetic susceptibility normalised to the number of spins

$$\frac{\chi(T)}{N} = \frac{\beta}{N}\left[\langle M^2 \rangle - \langle |M| \rangle^2\right]. \tag{A12}$$

$$\frac{\chi(T)}{N} = N\beta\left[\langle m^2 \rangle - \langle |m| \rangle^2\right]. \tag{A13}$$

Using these together with our previous results we can rewrite these equations, as shown in (A14).

$$\begin{aligned}\frac{\chi(T)}{N} &= 4\beta\left[\frac{2}{Z}\left(e^{8\beta J} + 1\right) - \left(\frac{2}{Z}(e^{8\beta J} + 2)\right)^2\right] \\ &= \frac{8\beta}{Z}\left[e^{8\beta J} + 1 - \frac{2}{Z}\left(e^{16\beta J} + 4e^{8\beta J} + 4\right)\right].\end{aligned} \tag{A14}$$